

An unsteady turbulent boundary layer

By STURE K. F. KARLSSON

Department of Aeronautics, The Johns Hopkins University

(Received 10 September 1958)

A low speed parallel flow, whose velocity fluctuates sinusoidally in magnitude about a constant mean, has been produced in a boundary layer wind tunnel. Hot-wire measuring techniques have been developed to permit an investigation of the turbulent boundary layer developing on a flat plate with this free stream condition. The response of the layer at a Reynolds number

$$R_{\delta^*} = (\bar{U}_\infty \delta^*)/\nu = 3.6 \times 10^3$$

was measured for free stream fluctuation amplitudes up to 34% of the mean velocity and frequencies ranging from 0 to 48 cycles/sec. Here $\delta^* = \int_0^\infty \left(1 - \frac{\bar{U}}{\bar{U}_\infty}\right) dy$ is the boundary displacement thickness, $\bar{U}(x, y)$ the mean velocity in the boundary layer, \bar{U}_∞ the mean velocity in the free stream, and ν the kinematic viscosity.

Measurements were made of the mean velocity, the amplitudes of in- and out-of-phase components of the first harmonic of the periodic fluctuations, and the intensity of higher harmonics and turbulence. It was found that non-linear effects, even at the largest fluctuation amplitudes, were so small that they were obscured by experimental errors.

Introduction

Many fluid flow problems are essentially unsteady in character. The flow over a turbine blade moving through the wakes of the guide vanes located upstream, or the flow over a rocket which accelerates from rest, are two typical examples. Problems such as these have in recent years stimulated a fair amount of interest in the behaviour of boundary layers subject to unsteady free stream conditions. In the investigation reported on here, a study was made of an unsteady turbulent boundary layer.

The ultimate goal of such a study is that it should enable one to predict the behaviour of the turbulent boundary layer at any instant, when the free stream is given as a function of time. The fact that the turbulent layer is a non-linear mechanism, however, makes this an exceedingly difficult problem. No longer can the responses due to a series of small changes of the input (free stream velocity) be superimposed to give the final response, as is the case in linear problems. In general, the unsteady turbulent boundary layer depends not only on the instantaneous value of the free stream velocity (among other things) but on its past history as well. Hence, knowledge of the response of the turbulent boundary layer to a specific kind of free stream fluctuation does not enable one, in general,

to predict the response to an arbitrary fluctuation of the free stream. Nevertheless, the best way to gain some initial understanding of this problem seems to be to study a situation, which is as simple and well defined as possible, with a specific fluctuation of free stream velocity with time.

The choice for the present experimental investigation was an incompressible two-dimensional turbulent boundary layer with a zero mean pressure gradient in the flow direction, where the free stream velocity fluctuated sinusoidally with amplitude u_∞ , say, and frequency $\omega/2\pi$, about a constant mean velocity \bar{U}_∞ .

General considerations

In interpreting the results of our measurements it will prove helpful to have some knowledge of the behaviour of the corresponding laminar layer. This problem, restricted to small free stream oscillations, has been treated by Light-hill (1954). Here we should like to learn something about the effects of non-linearity which will appear if the free stream fluctuations are large. This can be done by studying the response of the boundary layer to very slow (quasi-steady) fluctuations of free stream velocity. Then the velocity profile at any instant can be closely approximated by the steady profile corresponding to the instantaneous free stream velocity. For the boundary layer on a flat plate, the Blasius layer, the velocity is given by

$$U = U_\infty f' \left\{ y \sqrt{\left(\frac{U_\infty}{x\nu} \right)} \right\}, \tag{1}$$

where f is the Blasius function, x distance from leading edge in flow direction, y distance perpendicular to the plate, and ν kinematic viscosity.

U_∞ is the slowly varying free stream velocity $U_\infty(t)$, and the prime (') denotes differentiation with respect to the argument $\left\{ y \sqrt{\left(\frac{U_\infty}{x\nu} \right)} \right\}$.

Our interest is in the nature of the variations of U with time for a sinusoidal variation of U_∞ with time. To obtain an expression for this relationship which involves a minimum of other parameters, we multiply both sides of (1) by $y^2/x\nu$ and get

$$\frac{Uy^2}{x\nu} = \frac{U_\infty y^2}{x\nu} f' \left\{ y \sqrt{\left(\frac{\bar{U}_\infty}{x\nu} \right)} \right\}. \tag{2}$$

We put $Uy^2/x\nu = F$ and $U_\infty y^2/x\nu = n$. These are the only variables appearing in (2) and therefore the dependence upon the varying free stream velocity for the entire boundary layer is given by a single plot of F versus n of the form $F = nf'(\sqrt{n})$. This plot is shown in figure,1. The varying free stream velocity in our case is given by

$$U_\infty = \bar{U}_\infty(1 + \beta \cos \theta),$$

where θ is the slowly varying phase angle and $\bar{U}_\infty \beta$ the amplitude of the free stream fluctuations. Since U_∞ is directly proportional to n , we also have

$$n = n_\infty(1 + \beta \cos \theta),$$

and consequently

$$F = F[n_\infty(1 + \beta \cos \theta)]$$

is a function periodic in θ with period 2π . However, because of the non-linear nature of F the boundary layer velocity will not fluctuate sinusoidally with

a single frequency. Since F is symmetric with respect to $\theta = 0$ it can be expanded in a Fourier cosine series. For fixed values of n_∞ and β we have

$$F = \sum_{i=0}^{\infty} A_i \cos i\theta. \quad (3)$$

The first three of the Fourier coefficients A_i have been computed graphically as functions of n_∞ for $\beta = 0.3$ and 0.5 . After dividing both sides of (3) by $\bar{U}_\infty y^2/x\nu = n_\infty$, we get the expression for velocity in the boundary layer, i.e.

$$\frac{U}{\bar{U}_\infty} = \frac{A_0}{n_\infty} + \frac{A_1}{n_\infty} \cos \theta + \frac{A_2}{n_\infty} \cos 2\theta + \dots$$

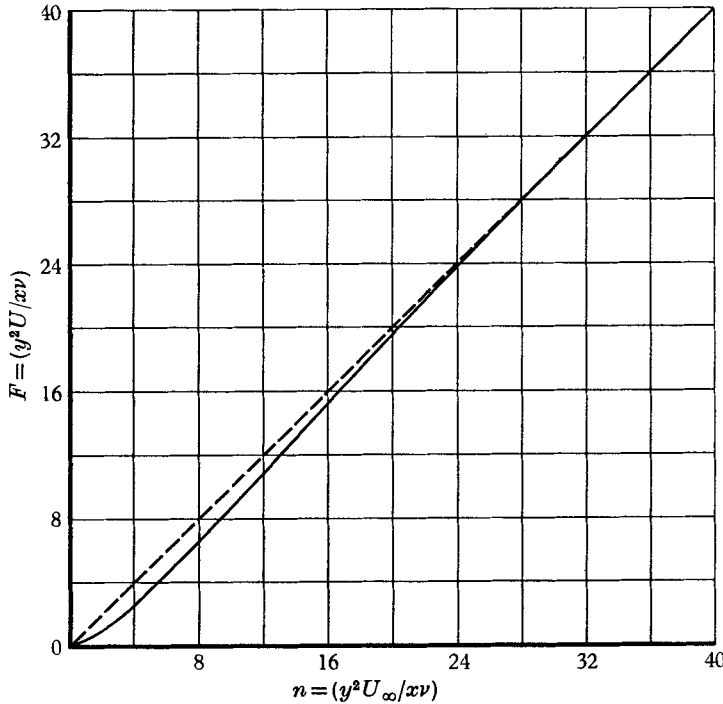


FIGURE 1. Transfer characteristic for the Blasius layer.

Using a different notation, we may write

$$\frac{U}{\bar{U}_\infty} = \frac{\bar{U}}{\bar{U}_\infty} + \frac{u^{(1)}}{\bar{U}_\infty} \cos \theta + \frac{u^{(2)}}{\bar{U}_\infty} \cos 2\theta + \dots$$

The quantities \bar{U}/\bar{U}_∞ , $u^{(1)}/\beta\bar{U}_\infty$, $u^{(2)}/\beta\bar{U}_\infty$ for $\beta = 0.3$ and 0.5 , and for comparison \bar{U}/\bar{U}_∞ and $u^{(1)}/\beta\bar{U}_\infty$ for $\beta \rightarrow 0$, have been plotted as functions of $\eta = \sqrt{n}$ in figure 2. These curves demonstrate the non-linear behaviour of the boundary layer with respect to slow free stream fluctuations. As the amplitude of these fluctuations is increased the mean velocity profile deviates progressively from the steady one. The slope of the profile at $\eta = 0$ and therefore also the skin friction increases with increasing amplitude.

Perhaps the most striking effect of non-linearity on the velocity fluctuations in the boundary layer is to produce higher harmonics, of which only the second has been plotted. We note that the sign of the amplitude of the second harmonic changes as we proceed from the plate to the edge of the boundary layer. This represents a 180° phase shift. Simultaneously the mean velocity for the oscillating boundary layer goes from a value which is greater than the corresponding steady velocity to one which is lower. It is remarkable, however, how small an effect the fluctuations have on the mean profile even for oscillations as great as 50% of the free stream.

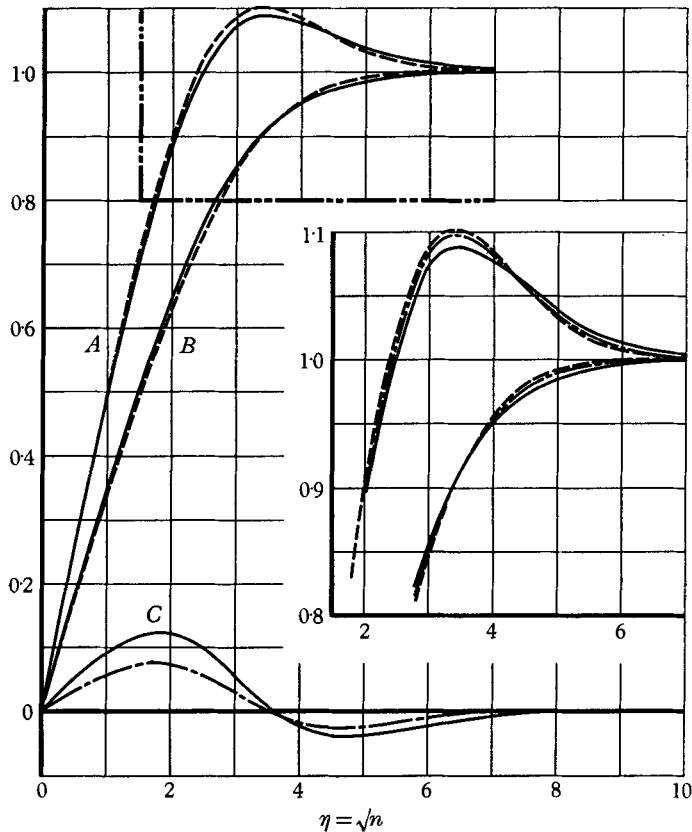


FIGURE 2. The quasi-steady Blasius layer. $A = u_1^{(1)}/\beta \bar{U}_\infty$, $B = \bar{u}/\bar{U}_\infty$, $C = u_2^{(2)}/\beta U_\infty$.
 - - - - $\beta = 0$, - - - - $\beta = 0.3$, - · - · $\beta = 0.5$.

From this quasi-steady analysis it is not possible to predict the behaviour of the layer subjected to large free stream oscillations of arbitrary frequency. But as in the case for small amplitude oscillations (Lighthill 1954), at very high frequency the periodic and mean motions become uncoupled (if compressibility effects can be neglected), the former being governed by a linear equation. As a result the higher harmonics disappear from the fluctuations in the boundary layer and the unsteady mean velocity profile becomes identical with the steady one.

Although the turbulent boundary layer is a much more complicated mechanism than the laminar layer, they are sufficiently related that it is possible to use some

of the results of the above laminar analysis to infer the qualitative behaviour of the turbulent layer. For instance, for the quasi-steady turbulent layer we should expect the fluctuation amplitude to have a maximum greater than the free stream amplitude located near the outer edge of the layer. Non-linear interaction between the mean velocity and the periodic fluctuations takes place here also, as in the laminar layer, if the fluctuation amplitude is large enough, and should result in an increase in skin friction and production of higher harmonics. Furthermore, at very high frequencies the (incompressible) fluctuations obey a linear equation and as a consequence the mean velocity profile in that case should be identical to the corresponding steady one.

The velocity fluctuations in the turbulent boundary layer subjected to free stream oscillations can be separated into two parts: periodic and random fluctuations. If the instantaneous free stream velocity is given by

$$U_{\infty}(t) = \bar{U}_{\infty} + \mathcal{R} \left(\sum_{n=1}^N u_{\infty}^{(n)} e^{in\omega t} \right), \quad (4)$$

where \bar{U}_{∞} is the constant mean velocity and the amplitudes $u_{\infty}^{(n)}$ are in general complex to indicate relative phase shifts between different frequencies, then for the velocities inside the boundary layer we can write

$$U_k(x_1, x_2, x_3, t) = \bar{U}_k(x_1, x_2) + \mathcal{R} \left[\sum_{n=1}^{\infty} u_k^{(n)}(x_1, x_2) e^{in\omega t} \right] + r_k(x_1, x_2, x_3, t). \quad (5)$$

The subscripts $k = 1, 2, 3$ represent the components along the three Cartesian co-ordinate axes x_1 , x_2 and x_3 , respectively, where x_1 is parallel to the solid surface in the direction of the flow and x_2 is normal to the surface. $r_k(x_1, x_2, x_3, t)$ is the random part of the velocity fluctuation. The complex amplitudes are defined by

$$u_k^{(n)}(x_1, x_2) = 2 \overline{U_k(x_1, x_2, x_3, t) e^{-in\omega t}}, \quad (6)$$

where the bar means a double averaging process: the ensemble average of the time average over a complete cycle of periodic fluctuation. That is,

$$\overline{U_k e^{-in\omega t}} \equiv \lim_{N \rightarrow \infty} \frac{1}{N} \sum_{l=1}^N \frac{\omega}{2\pi} \int_0^{2\pi} U_{kl} e^{-in\omega t} dt, \quad (7)$$

where U_{kl} is a particular realization of the velocity. By substituting (5) into the equations of motion we can obtain the boundary-layer equations for the mean velocity, periodic amplitudes and turbulence intensity. These equations are given in the author's dissertation (Karlsson 1958).

The experimental techniques used in the present experiments permitted the measurement of only the first harmonic of the periodic fluctuations. Consequently, it was necessary in the experiment to separate the fluctuations in a slightly different way than outlined above. The higher harmonics of the periodic fluctuations were added to the turbulence and the root-mean-square value of this sum was measured. This is not a serious shortcoming, since the free stream fluctuations consisted essentially of a single frequency and the higher harmonics produced in the boundary layer due to non-linear interactions (as it turned out) must have been quite small.

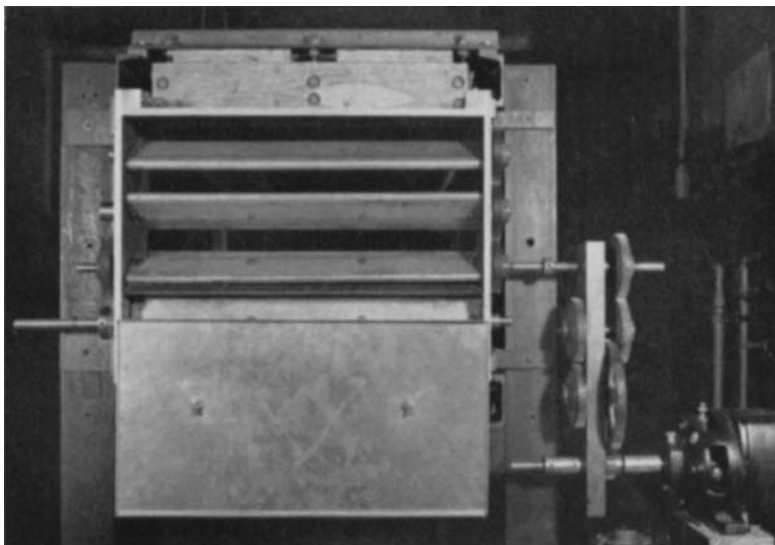


FIGURE 4 (plate 1). Shutter for producing sinusoidal fluctuations.

Experimental equipment

The wind tunnel. The unsteady boundary-layer measurements were made in the boundary layer developing on the floor in the wind tunnel described by Johnson (1957). To accomplish the free stream fluctuations the exit area of the test section was varied by means of a shutter consisting of four parallel rotating vanes driven by an electric motor. The frequency of the free stream fluctuations could be varied continuously from $\frac{1}{3}$ to 60 cycles/sec. A schematic side view of the wind tunnel and a photograph of the shutter are shown in figure 3 and in figure 4, plate 1.

The free stream fluctuations were very nearly sinusoidal at the frequencies for which measurements were performed, except at the highest frequency, where the higher harmonics (primarily second) accounted for about 15% of the total root-mean-square amplitude. From the acoustic point of view the fluctuations at the lower frequencies, 0.33 to 4 cycles/sec, were quasi-steady. However, as 8 cycles/sec was approached a parasitic third harmonic gained in amplitude due to acoustic reflexion. 24 cycles/sec was the fundamental frequency for the standing sound wave with pressure nodes at the beginning and end of the test section and

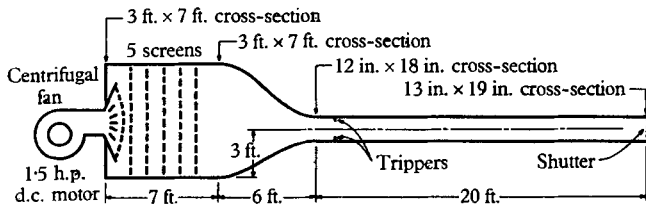


FIGURE 3. Sketch of wind tunnel.

Screen	Mesh	Solidity
1	30	0.63
2, 3	10	0.43
4	36	0.42
5	43	0.38

a velocity node in the middle. Since the measurements were performed near the middle and large fluctuations were desired, this frequency was not suitable for measurements. But measurements were performed at 48 cycles/sec, which is the second harmonic. Then there was a velocity loop in the middle of the test section with nodes on either side, halfway between the middle- and the end-points.

To remove objectionable vibration induced by the oscillating pressure it was necessary to reinforce the floor and the ceiling of the test section. After this improvement the maximum deflexion anywhere on the floor or ceiling was less than 0.001 in. relative to the externally supported hot-wire probe.

An efficient tripping device was installed, which insured transition from laminar to turbulent boundary-layer flow at the same location for the entire range of velocities used in the experiments.

The pressure gradient in the flow direction was very nearly zero in the test section for steady operation of the wind tunnel at both minimum and maximum speeds. The variation of static pressure was within $\pm 0.4\%$ of $\frac{1}{2}(\rho \bar{U}_\infty^2)$, the dynamic pressure in the free stream ($\rho =$ density of air).

Hot-wire equipment. Two hot-wire probes were used simultaneously for the unsteady boundary-layer measurements, one stationary in the free stream and one traversing the boundary layer. The traversing gear used for this probe was the same as that described by Johnson (1957). Both probes were placed centrally with respect to the side walls of the test section. Their longitudinal position could be varied over the entire 20 ft. long test section.

Throughout these experiments, 0.0001 in. diameter straight platinum hot-wires were used having a cold resistance of about 17 Ω . The heating current was adjusted so that the hot resistance was 1.8 times this value.

A new constant temperature transistor hot-wire set, recently developed by Kovaszny (1958), was employed in this work. This set has a fully compensated response from d.c. up to about 17,000 cycles/sec, which is the frequency for free oscillations, characteristic for constant temperature hot-wire sets under certain operating conditions (Kovaszny 1948). The great advantage with a constant temperature hot-wire set is that it is properly compensated even for large fluctuations in velocity. Furthermore, it is relatively easy to operate on its output signal in such a way that the final output is directly proportional to velocity.

King's equation, which expresses the heat balance in the hot-wire, can for this case be written very simply

$$U = (aI^2 - b)^2, \quad (8)$$

where U is the velocity, I the current, and a and b are dimensional constants which depend upon operating conditions and wire properties. The output voltage of the constant current hot-wire set is proportional to I . Hence, to get a signal which is proportional to the velocity it is necessary to square the output voltage, subtract a constant bias voltage, then square again. The bias is set so that the final output is zero for zero velocity. This procedure was followed here, using Philbrick multipliers for squaring circuits. Actually, equation (8) is not strictly true for very low velocities, but it was found that linear response could be obtained by this method over the range of velocity of interest.

Total head tube-manometer. For the purpose of hot-wire calibration the velocity in the wind tunnel was measured with a total head tube. The difference between total head and static pressure as sensed by a static tap in the floor was measured with a 10:1 inclined manometer. The possible error in this measurement was conservatively ± 0.0004 in. alcohol, corresponding to a maximum possible error in velocity of $\pm 1\%$ at the lowest speed measured. The pitot tube was not used for mean velocity measurements in the unsteady boundary layer, since it did not behave reliably when subjected to large velocity fluctuations.

Measuring techniques

The circuitry used for processing the linearized hot-wire signals is shown in a simplified diagram in figure 5. Since the output voltage of the hot-wire sets are proportional to the velocities, the same notation has been used for voltages as for velocities.

At low frequencies of periodic fluctuation the mean velocities could not be measured directly at the output of the hot-wire sets because of the large meter fluctuations. The necessary averaging was accomplished with a simple RC net-

work which had a time constant of about one second. Owing to the finite impedance of the vacuum tube volt meter, a correction of about +4% had to be applied to this reading.

The velocity fluctuations in the boundary layer are conveniently separated into two parts: (a) the fundamental frequency of the periodic fluctuation, and (b) the turbulence and higher harmonics generated through non-linear interaction.

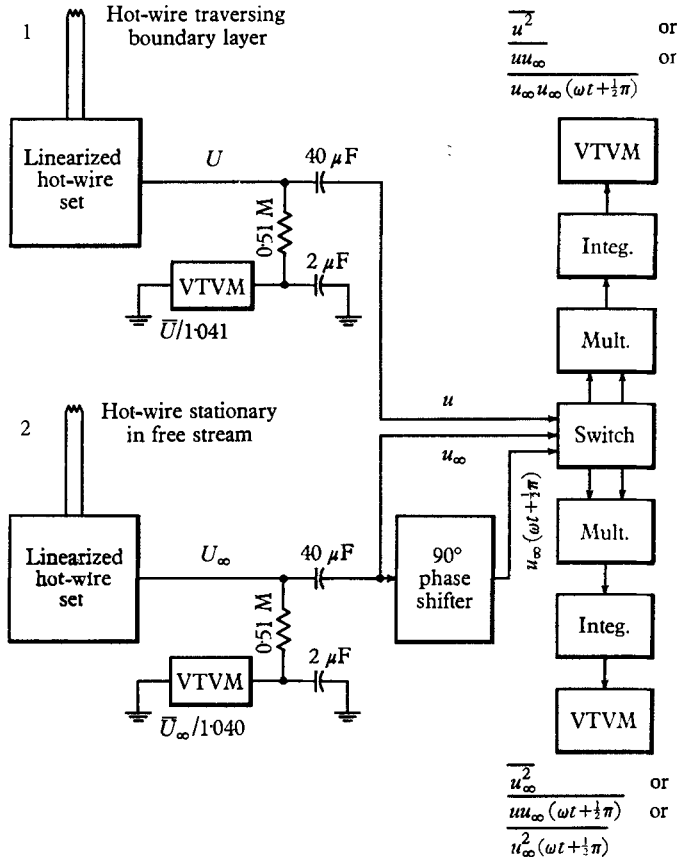


FIGURE 5. The hot-wire output circuit, VTVM = vacuum tube volt meter.

If the fluctuations in the free stream are

$$u_\infty = u_\infty^{(1)} \cos \omega t, \tag{9}$$

then inside the boundary layer the fluctuations in the x -direction are

$$\begin{aligned} u(x, y, z, t) &= u^{(1)}(x, y) \cos [\omega t + \phi(x, y)] + r(x, y, z, t) \\ &= u^{(1)} \cos \phi \cos \omega t - u^{(1)} \sin \phi \sin \omega t + r, \end{aligned} \tag{10}$$

where r contains higher harmonics as well as the random fluctuations. Multiplying with the free stream fluctuations and averaging, one gets

$$\overline{u_\infty u} = \frac{u_\infty^{(1)} u^{(1)} \cos \phi}{2}. \tag{11}$$

After shifting the free stream oscillation through 90° , multiplying and averaging, we have

$$\overline{u_\infty(\omega t + \frac{1}{2}\pi)u} = \frac{u_\infty^{(1)}u^{(1)}\sin\phi}{2}. \quad (12)$$

The amplitudes of the in- and out-of-phase components of the boundary-layer fluctuations are then respectively

$$u^{(1)}\cos\phi = \sqrt{2} \frac{\overline{u_\infty u}}{(\overline{u_\infty^2})^{\frac{1}{2}}} \quad (13)$$

and

$$u^{(1)}\sin\phi = \sqrt{2} \frac{\overline{u_\infty(\omega t + \frac{1}{2}\pi)u}}{(\overline{u_\infty^2})^{\frac{1}{2}}}. \quad (14)$$

The mean square of the total boundary-layer fluctuation is given by

$$\overline{u^2} = \frac{\overline{u^{(1)2}}}{2} + \overline{r^2}, \quad (15)$$

since r is uncorrelated with the rest of the signal. Solving for $\overline{r^2}$, we have finally

$$\overline{r^2} = \overline{u^2} - \left[\frac{(\overline{u_\infty u})^2}{\overline{u_\infty^2}} + \frac{(\overline{u_\infty(\omega t + \frac{1}{2}\pi)u})^2}{\overline{u_\infty^2}} \right]. \quad (16)$$

The mean products $\overline{u^2}$, $\overline{u_\infty^2}$, $\overline{u_\infty u}$ and $\overline{u_\infty(\omega t + \frac{1}{2}\pi)u}$ were computed electronically by the network shown in figure 5. The components of the computing network employed Philbrick-type, operational amplifiers and the multipliers were Philbrick GAP/R MODEL MU/DV.

Measurements

Except for preliminary surveys, the majority of the measurements were made at a distance of 98 in. from the boundary-layer tripping device. However, the 48 cycles/sec measurements were made at 114 in.

The free stream mean velocity was approximately 17.5 ft./sec for all experiments, except for 0.33 cycles/sec and the quasi-steady case, which were carried out at a mean velocity of 15 ft./sec. In either case the turbulent boundary-layer thickness was approximately 3 in. and the Reynolds number based on the free stream mean velocity and boundary displacement thickness was about 3.6×10^3 . At 17.5 ft./sec the local skin friction coefficient, c_f , was approximately 0.0034, as determined by the 'law of the wall' (Clauser 1954).

Boundary-layer measurements were carried out at the following frequencies: 0 (quasi-steady), 0.33, 0.66, 1, 1.33, 2, 4, 7.65 and 48 cycles/sec. At each frequency, except 0 and 48 cycles/sec, measurements were made at free stream fluctuation amplitudes varying from about 8 to 34 % of the free stream mean velocity. For 0 and 48 cycles/sec, results were obtained for single free stream amplitudes of 30 and 34 %, respectively. The quantities measured during each boundary layer survey were mean velocity, amplitudes of in- and out-of-phase components of the fundamental frequency and turbulence intensity level. The experimental results are plotted in figures 6 to 14.

The quasi-steady or slowly oscillating case was computed graphically from a series of steady boundary-layer measurements, following in principle the same procedures as for the laminar case discussed previously. The results for the turbu-

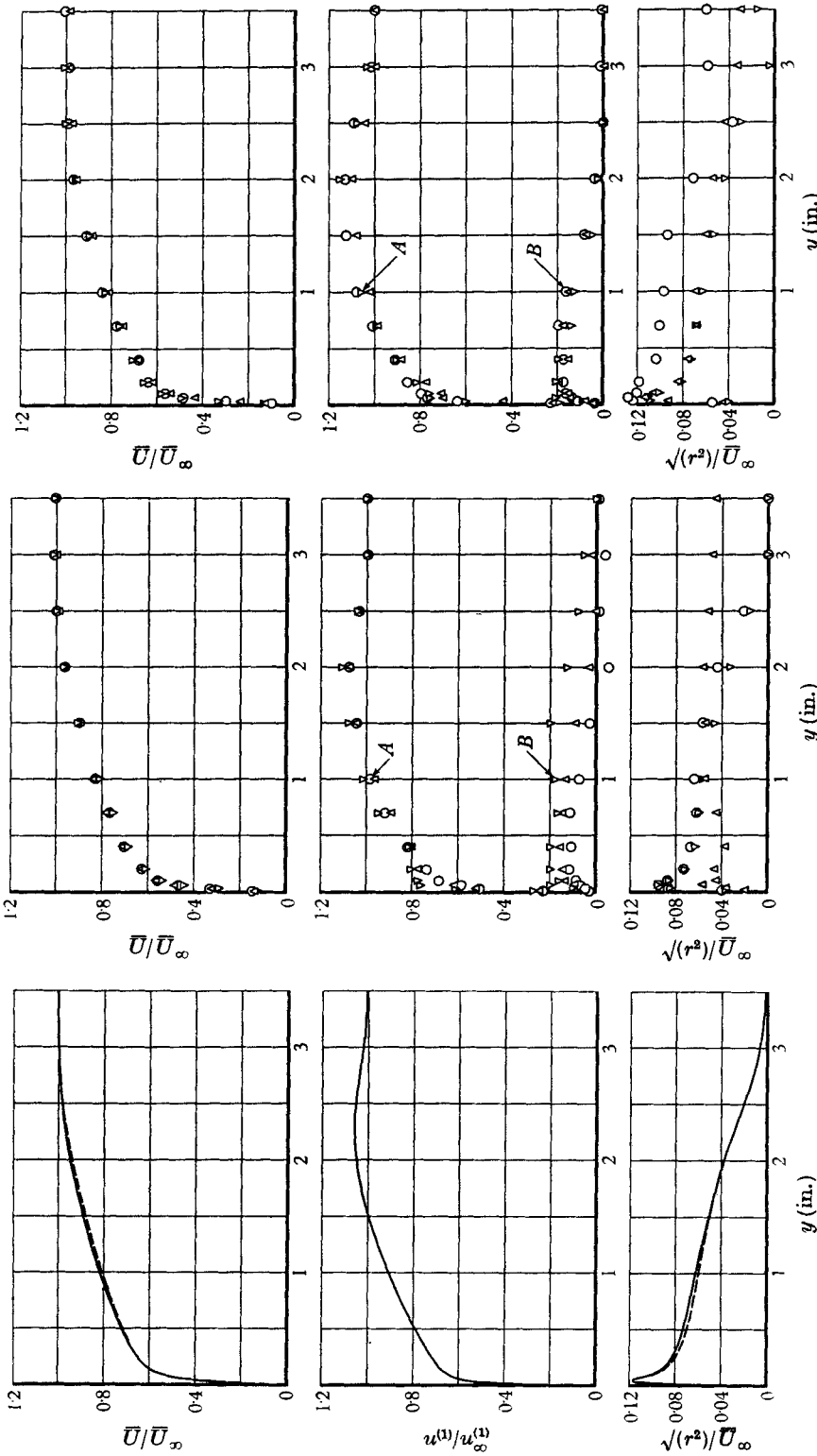


FIGURE 6

FIGURE 7

FIGURE 8

FIGURE 6. The quasi-steady (slowly varying) turbulent layer. $u_\infty^{(1)}/\bar{U}_\infty = 30\%$, $u_\infty^{(1)}/\bar{U}_\infty = 0$.
 FIGURE 7. Results for the unsteady turbulent layer. $\omega/2\pi = 0.33$ cycles/sec; $u_\infty^{(1)}/\bar{U}_\infty = 29.2\%$ (Δ), 14.7% (∇). $A = u^{(1)} \cos \phi/u_\infty^{(1)}$, $B = u^{(1)} \sin \phi/u_\infty^{(1)}$.
 FIGURE 8. Results for the unsteady turbulent layer. $\omega/2\pi = 0.66$ cycles/sec; $u_\infty^{(1)}/\bar{U}_\infty = 34.0\%$ (\circ), 14.9% (Δ), 11.2% (∇). $A = u^{(1)} \cos \phi/u_\infty^{(1)}$, $B = u^{(1)} \sin \phi/u_\infty^{(1)}$.

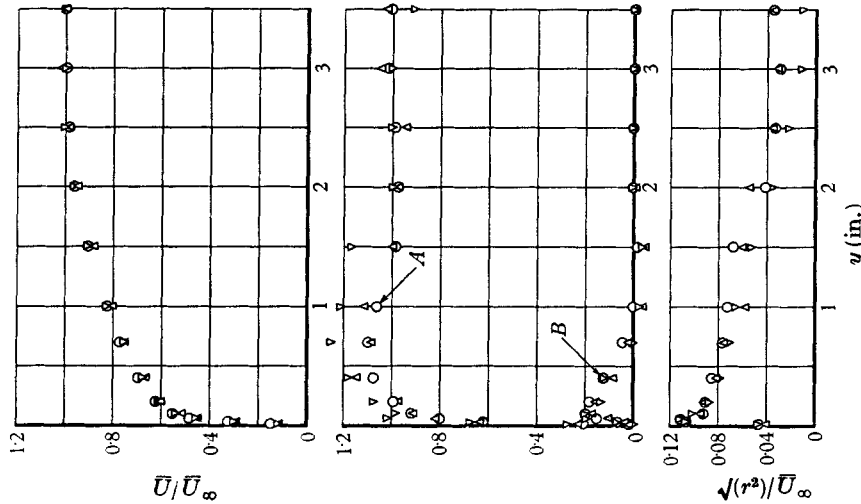


FIGURE 11

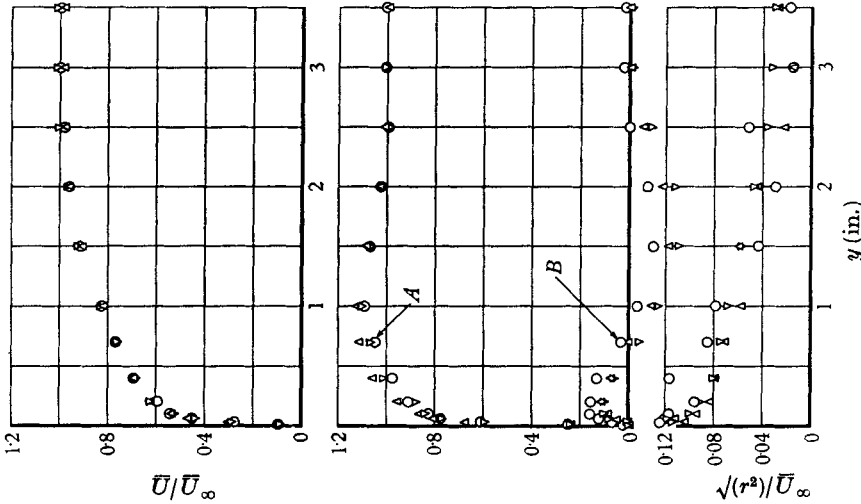


FIGURE 10

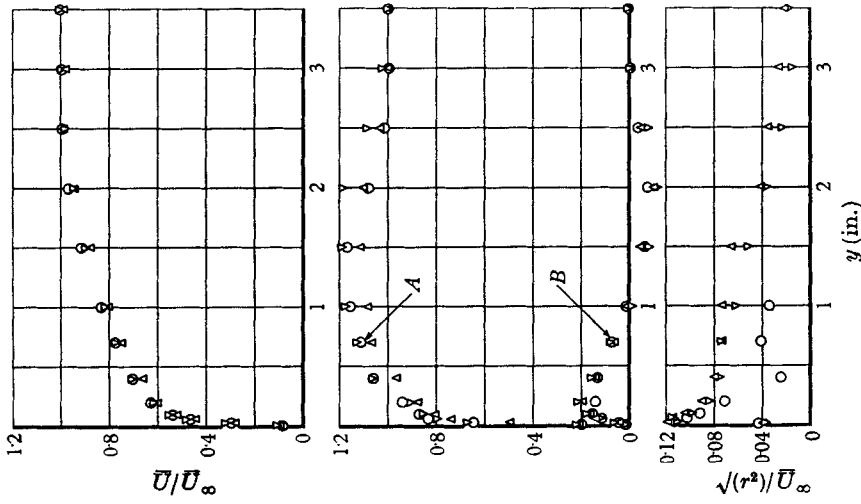


FIGURE 9

FIGURE 9. Results for the unsteady turbulent layer. $\omega/2\pi = 1.0$ cycles/sec; $u_\infty^{(1)}/\bar{U}_\infty = 35.2\%$ (O), 19.5% (Δ), 10.7% (∇). $A = u^{(1)} \cos \phi / u_\infty^{(1)}$, $B = u^{(1)} \sin \phi / u_\infty^{(1)}$.
 FIGURE 10. Results for the unsteady turbulent layer. $\omega/2\pi = 1.33$ cycles/sec; $u_\infty^{(1)}/\bar{U}_\infty = 34.4\%$ (O), 21.5% (Δ), 13.0% (∇). $A = u^{(1)} \cos \phi / u_\infty^{(1)}$, $B = u^{(1)} \sin \phi / u_\infty^{(1)}$.
 FIGURE 11. Results for the unsteady turbulent layer. $\omega/2\pi = 2.0$ cycles/sec; $u_\infty^{(1)}/\bar{U}_\infty = 28.6\%$ (O), 17.6% (Δ), 8.1% (∇). $A = u^{(1)} \cos \phi / u_\infty^{(1)}$, $B = u^{(1)} \sin \phi / u_\infty^{(1)}$.

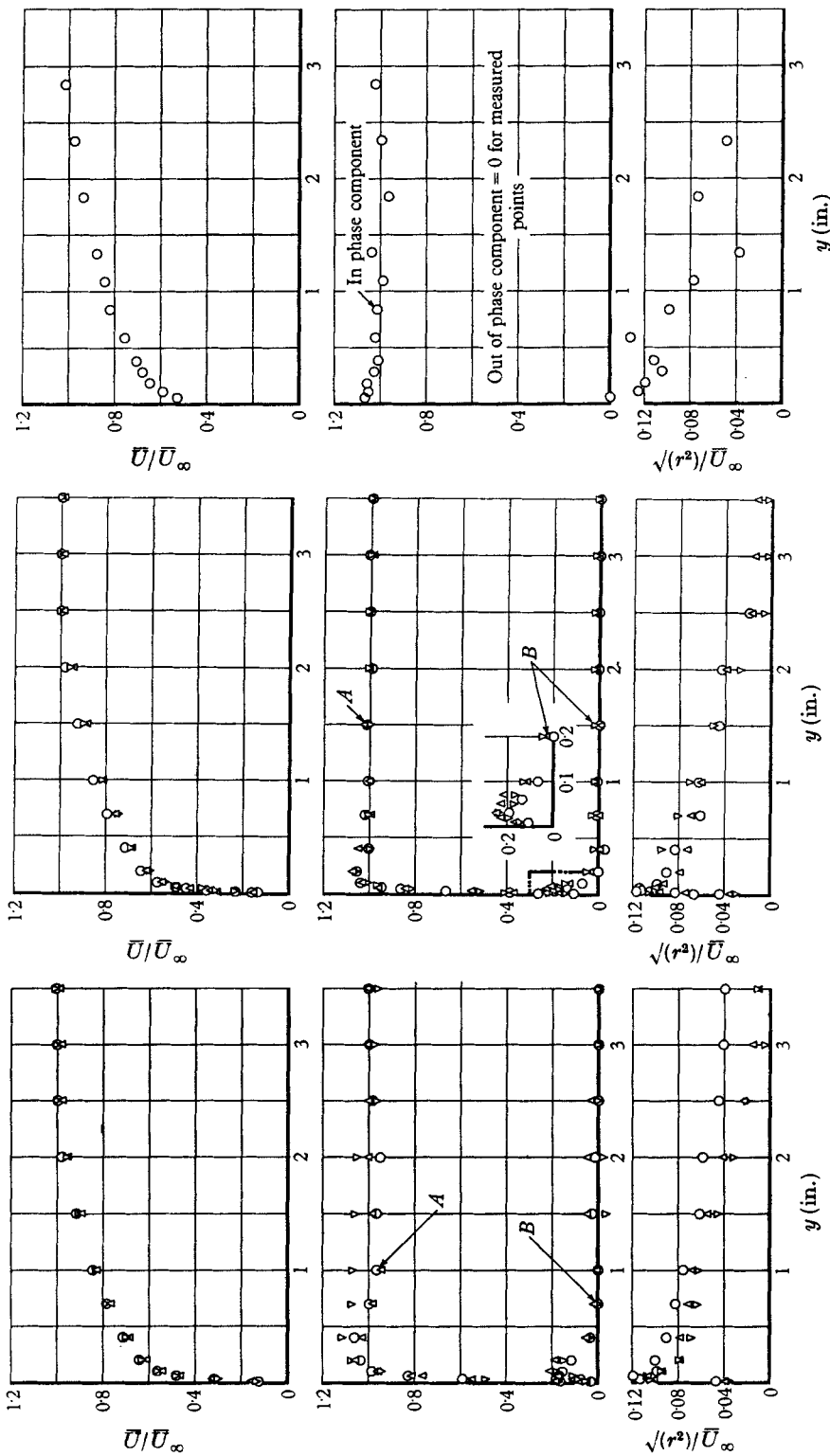


FIGURE 12

FIGURE 13

FIGURE 14

FIGURE 12. Results for the unsteady turbulent layer. $\omega/2\pi = 4.0$ cycles/sec; $u_\infty^{(1)}/\bar{U}_\infty = 26.4\%$ (\circ), 13.6% (Δ), 6.2% (∇). $A = u^{(1)} \cos \phi/u_\infty^{(1)}$, $B = u^{(1)} \sin \phi/u_\infty^{(1)}$.

FIGURE 13. Results for the unsteady turbulent layer. $\omega/2\pi = 7.65$ cycles/sec; $u_\infty^{(1)}/\bar{U}_\infty = 29.7\%$ (\circ), 12.7% (Δ), 7.3% (∇). $A = u^{(1)} \cos \phi/u_\infty^{(1)}$, $B = u^{(1)} \sin \phi/u_\infty^{(1)}$.

FIGURE 14. Results for the unsteady turbulent layer. $\omega/2\pi = 48$ cycles/sec; $u_\infty^{(1)}/\bar{U}_\infty = 34\%$ (\circ).

lent layer are shown in figure 6 along with the profile whose free stream velocity is the same as the mean for the oscillating case. A comparison between the two profiles points out the interesting fact that the effect of non-linearity in the quasi-steady case is to *increase* the mean velocity over the major part of the profile! This gives the appearance of a thinner boundary layer and actually the displacement and momentum thicknesses are less than for the steady layer. However, although it does not show up very clearly on the graph, the mean profile is somewhat thicker and the mean shear stress at the wall is 4% greater than in the steady case. The amplitude of the sinusoidal fluctuations increases very rapidly near the wall, then at a slower rate and reaches a maximum not far from the outer edge of the boundary layer. Non-linear effects on the fundamental frequency are almost nil at this amplitude. A slight effect is observed on the turbulence level.

For the unsteady boundary layer, figures 7 to 14, no systematic variation in the mean velocity profiles with fluctuation amplitude or frequency can be detected. This is really not so surprising, in view of the remarkably small effect on non-linearity on the quasi-steady profile.

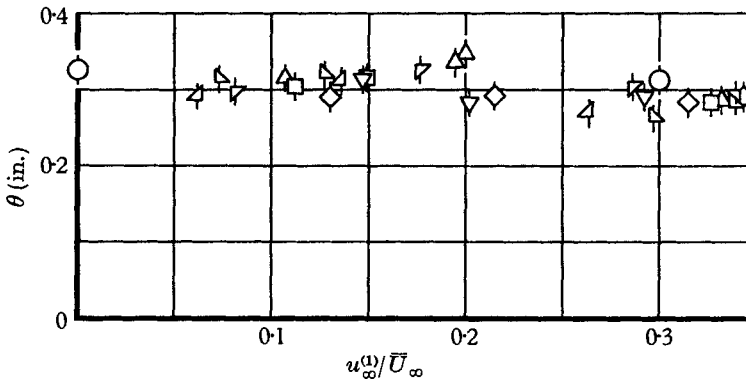


FIGURE 15. The momentum thickness (cycles/sec): \circ , Quasi-steady; ∇ , 0.33; \square , 0.66; \triangle , 1.0; \diamond , 1.33; ∇ , 2.0; \triangle , 4.0; \triangle , 7.65; ∇ , 48.0.

Unfortunately, hot-wire measurements of this kind are plagued with sizeable random as well as systematic errors. A somewhat conservative estimate of the maximum possible error in the mean velocity profile is $\pm 2\%$, of which half may be due to the uncertainty in the calibration of the hot-wires. The existence of this last error is in evidence at the outer edge of some of the profiles, which do not approach 1.0 exactly, although the stationary and traversing wires are measuring the same velocity.

In view of this we cannot state accurately what the effect of free stream oscillations are on the mean velocity profile. However, we can draw the following important conclusion. The change in the mean velocity profile is quite small, even when the fluctuation amplitude in the free stream is as high as 30%.

The momentum thickness, $\theta = \int_0^\infty \frac{\bar{U}}{\bar{U}_\infty} \left(1 - \frac{\bar{U}}{\bar{U}_\infty}\right) dy$, of the mean profiles has been plotted in figure 15 versus the free stream fluctuation amplitude. The vertical lines

through the points indicate the possible deviation due to a ± 0.01 systematic error in the mean profile.

The in-phase $\{(u^{(1)}/u_{\infty}^{(1)}) \cos \phi\}$ and out-of-phase $\{(u^{(1)}/u_{\infty}^{(1)}) \sin \phi\}$ components of the first harmonic of the boundary-layer fluctuations are also plotted in figures 7 to 14. It is estimated that the possible error in these measurements is about $\pm 5\%$ of the free stream fluctuation amplitude. The error is partly systematic, partly random. The reason for the large relative error for the out-of-phase component is primarily the difficulty in averaging this quantity, which has large, slow fluctuations.

Nevertheless, the measurements give a good description of the behaviour of the periodic fluctuations throughout the boundary layer and for different frequencies. At the lowest frequency of 0.33 cycle/sec, the in-phase component is very nearly the same as the amplitude of the quasi-steady oscillations. However, a positive out-of-phase component has also developed, indicating that the oscillations in the boundary layer are ahead of those in the free stream. This agrees with the behaviour of the corresponding laminar boundary layer. As pointed out by Lighthill (1954) such a phase advance in the boundary layer is to be expected, since the fluctuating pressure gradient acting on the slow moving fluid in the boundary layer is the same as the one necessary to accelerate the free stream. The same acceleration results in a greater relative change of velocity in the boundary layer than in the free stream.

The effect of increasing frequency upon the in-phase component of fluctuation amplitude is to bring the maximum value closer to the wall. The out-of-phase component becomes negative for the outer portion of the boundary layer at 1 cycle/sec, indicating that there is a lag in the fluctuations here relative to the free stream. This lag is still present at 1.33 cycles/sec, but for higher frequencies it is decreased and eventually disappears, as the region over which the fluctuations are affected by the presence of the wall becomes thinner. For the region close to the wall the out-of-phase component is positive for all the frequencies. The largest measured phase shift occurs at 7.65 cycles/sec and is approximately 35° at $y = 0.010$ in., which is well within the laminar sublayer. A consistent effect of amplitude cannot be detected, and one must conclude that this effect is so small that it is obscured by the experimental errors.

At 48 cycles/sec the periodic fluctuations differ from those in the free stream only in a very thin layer near the wall. For this frequency the 'Rayleigh thickness', $\sqrt{(2\nu/\omega)}$, is about 0.012 in. This is less than half of the laminar sublayer thickness, which is here approximately 0.030 in. Comparing this case with that treated by Lighthill (1954), we may expect that the fluctuations are of the 'shear wave' type. It was not possible to check this experimentally, because the flow was reversed in direction during part of the period from $y = 0$ to about $y = 0.030$ in. Since the hot-wire anemometer senses only magnitude of velocity, it cannot be used effectively to gain quantitative information about a flow that has reversals in velocity.

The measured turbulence intensity (and higher harmonics) is shown at the bottom of figures 7 to 14. The accuracy of these results is rather poor, since they are obtained by subtracting two quantities that are usually considerably larger

than the difference. This is especially true for the outer portion of the layer. In the vicinity of the wall, where the turbulence intensity is greatest, the estimated possible error is $\pm 8\%$. Within these limits the maximum turbulence level measured for the oscillating case agrees with the steady layer.

Conclusion

The experimental investigation of the zero-pressure gradient-turbulent boundary layer with a sinusoidally fluctuating free stream was intended as an initial effort in the study of unsteady turbulent boundary layers. One of the most remarkable results of this work was that the effect due to non-linear interaction was quite small, even for fluctuation amplitudes as large as 34% of the free stream velocity. Hence, transient zero-pressure gradient boundary layers, which at any given instant do not deviate very much from the steady layer, corresponding to the instantaneous free stream velocity, can be predicted using linear methods. To perform this computation it is sufficient to know the response of the layer to small sinusoidal free stream fluctuations at all frequencies. The measurements here give this response for a Reynolds number of $R_x^* \sim 3.6 \times 10^3$.

The author wishes to express his appreciation to Dr F. H. Clauser, who through many helpful suggestions contributed greatly to the accomplishment of this work, and to Dr M. V. Morkovin for many stimulating discussions.

This investigation was supported by the Flight Propulsion Laboratory Department, General Electric Company, Cincinnati, Ohio.

REFERENCES

- CLAUSER, F. H. 1954 Turbulent boundary layers in adverse pressure gradients. *J. Aero Sci.* **21**, 91.
- JOHNSON, D. S. 1957 Velocity, temperature and heat-transfer measurements in a turbulent boundary layer downstream of a stepwise discontinuity in wall temperature. *J. Appl. Mech.* **24**, 2.
- KARLSSON, S. K. F. 1958 *An unsteady turbulent boundary layer*. Doctoral thesis. Department of Aeronautics, Johns Hopkins University.
- KOVASZNAY, L. S. G. 1948 *Simple analysis of the constant temperature hot-wire anemometer*. Department of Aeronautics, Johns Hopkins University.
- KOVASZNAY, L. S. G. 1958 SQUID project. *Semi-Annual Progress Report* (April 1, 1958), Johns Hopkins University.
- LIGHTHILL, M. J. 1954 The response of laminar skin friction and heat transfer to fluctuations in stream velocity. *Proc. Roy. Soc. A*, **224**, 1.